Naval Research Laboratory

Washington, DC 20375-5320

NRL/MR/7620--95-7738

Uncertainties in Reflectance Measurements Made on the NRL Beam Line X24C

M.P. KOWALSKI
R.G. CRUDDACE
J.F. SEELY
J.C. RIFE

X-Ray Astronomy Branch
Space Science Division

July 17, 1995

REPORT DOCUMENTATION PAGE

Form Approved
OMB No. 0704-0188

1. AGENCY USE ONLY (*Leave Blank*)	2. REPORT DATE	3. REPORT TYPE AND DATES COVERED
	July 17, 1995	Memorandum Report

4. TITLE AND SUBTITLE

Uncertainties in Reflectance Measurements Made on the NRL Beam Line X24C

5. FUNDING NUMBERS

6. AUTHOR(S)

M.P. Kowalski, R.G. Cruddace, J.F. Seely, J.C. Rife, and W.R. Hunter*

7. PERFORMING ORGANIZATION NAME(S) AND ADDRESS(ES)

Naval Research Laboratory
Washington, DC 20375-5320

8. PERFORMING ORGANIZATION REPORT NUMBER

NRL/MR/7620--95-7738

9. SPONSORING/MONITORING AGENCY NAME(S) AND ADDRESS(ES)

Office of Naval Research
Arlington, VA 22217

10. SPONSORING/MONITORING AGENCY REPORT NUMBER

11. SUPPLEMENTARY NOTES

*SAF, Inc., Landover, MD

12a. DISTRIBUTION/AVAILABILITY STATEMENT

Approved for public release distributon unlimited.

12b. DISTRIBUTION CODE

13. ABSTRACT (*Maximum 200 words*)

A comprehensive attempt has been made to identify and quantify sources of uncertainty associated with measurements made with the reflectometer on the NRL beam line X24C. Measuremental uncertainty is dominated by angular reproducibility in the reflectometer and the stability of the electron beam. At wavelengths near the silicon L edge, the error in wavelength scale, set by the monochromator, is about 0.3 Angstroms. In samples with good signal-to-noise, the error in the reflectance is about 1% of the value of the reflectance. The error is correlated with the slope of the reflectance profile, varying between 1% of the reflectance value where the slope is flat to 10% of the reflectance value where the slope is steep.

14. SUBJECT TERMS

Optics
Extreme-ultraviolet
Instrumentation

15. NUMBER OF PAGES

27

16. PRICE CODE

17. SECURITY CLASSIFICATION OF REPORT	18. SECURITY CLASSIFICATION OF THIS PAGE	19. SECURITY CLASSIFICATION OF ABSTRACT	20. LIMITATION OF ABSTRACT
UNCLASSIFIED	UNCLASSIFIED	UNCLASSIFIED	SAR

NSN 7540-01-280-5500

Standard Form 298 (Rev. 2-89)
Prescribed by ANSI Std 239-18
298-102

CONTENTS

UNCERTAINTIES IN REFLECTANCE MEASUREMENTS MADE ON THE NRL BEAM LINE X24C

INTRODUCTION

The Naval Research Laboratory operates beam line X24C of the National Synchrotron Light Source at the Brookhaven National Laboratory. This beam line is equipped with a dual element grating/crystal monochromator (Rife, Hunter, & Williams 1986; Rife, Sadeghi, & Hunter 1989) which focuses monochromatized synchrotron light into an experimental chamber. Currently two such chambers are in use, the first being devoted to surface analysis measurements and the second being a reflectometer (Hunter & Rife 1986). (The reader is encouraged to read the references and will find them very useful in understanding the internal components of the monochromator and reflectometer, which are referred to throughout this paper.)

The reflectometer has been used in a wide variety of studies, including reflectance measurements of multilayer mirrors (Barbee et al. 1993; Seely et al. 1993a) and crystals (Chen & Hunter 1995), efficiency measurements of multilayer gratings (Cruddace et al. 1990; Kowalski et al. 1993; Seely et al. 1993b), photoluminescence measurements of phosphors (Schnatterly et al. 1995), and transmission measurements of thin films (Seely et al. 1992). However, no systematic determination has been made yet of the uncertainties associated with these measurments. This report describes a comprehensive attempt to determine and quantify the sources of experimental uncertainty.

The test sample is described first. Then, to understand fully the sources of measurement uncertainty, it is necessary to describe in detail both the experimental setup and the sample measurement procedure. Potential sources of measurement uncertainty are then identified, and the results of a series of tests designed to quantify uncertainties are discussed.

Manuscript approved May 17, 1995.

SAMPLE

The primary sample used for this study was a multilayer-coated mirror. The Mo/Si multilayer was designed to have peak near-normal incidence reflectance at a wavelength of 130 Angstroms. The deposition conditions were adjusted for an expected layer period of 67.5 Angstroms and a ratio of Mo layer thickness to layer period of 0.23. During the deposition run, 35 periods of Mo and Si were deposited onto a superpolished (1 Angstrom RMS roughness) flat mirror of diameter 25 mm and thickness 6 mm. The top layer was Mo, and a carbon overcoat of thickness 10 Angstroms was applied to minimize front surface oxidation. This sample was coated as part of a broader program to investigate the use of multilayers on diffraction gratings. The results of that study, including the measured reflectance of this sample, are discussed in detail in Barbee et al. (1993) and Kowalski et al. (1995).

Although the measurement procedure may vary slightly from sample to sample, reflectance measurements in p-polarization of a multilayer mirror sample constitute a good illustrative case given the past uses of the reflectometer. More importantly, the peak wavelength of a multilayer's response is a sinusoidal function of the incident radiation's grazing angle as determined by the Bragg equation. Thus, a multilayer sample can be used as a sensitive diagnostic tool to ascertain uncertainties in this angle. For example, at a grazing angle of 80° a shift of 0.1 eV in the peak energy of the test sample corresponds to a change of 0.2° in the angle of incidence. Finally, although multilayers may degrade with time if stored in air, they are stable over the short time period of this study. The measured peak reflectance of the test sample was 54.8% shortly after fabrication and decreased to 42.3% in 4.5 years as a consequence of carbon contamination and oxidation. Within the limits of uncertainty discussed in this article, the peak energy did not change. The most recent measurement was conducted three months before the present study.

EXPERIMENTAL SETUP

In the monochromator, the first and second optical elements may be selected from carousels which contain six optics. For the measurements described here, the first monochromater element was a gold-coated mirror, and the second monochromator element was a 600 g/mm grating with a blaze angle of 2.0°. The monochromator wavelength may be varied using a number of scan modes which include on-blaze and off-blaze motions of the elements. Only on-blaze scans were made for this study. For a wavelength of 130 Angstroms (energy 95.4 eV) the synchrotron light reflects off the monochromator elements at a grazing angle of approximately 3.6°, and the resolution is about 400 (0.25 eV).

Unbacked transmission filters are used to suppress radiation from orders higher than one that are produced by the monochromator gratings. A wide variety of filter materials and thicknesses are available. These filters are located on a vertical transport mechanism and intercept the direct beam just upstream of the exit slit. For this study, a silicon filter of thickness 2000 Angstroms was chosen.

The exit slit is located at the entrance to the reflectometer. This assembly restricts the beam to a fixed width of approximately 1 mm and a height of up to 2 mm (in the monochromator dispersion direction) depending upon the position of a pair of adjustable slit jaws. Thus for measurements of p-polarized light, the synchrotron light footprint subtends the entire horizontal width of the sample at shallow grazing angles, but decreases to 1 mm at normal incidence. For this study, the adjustable slit jaws were set at a separation of 400 microns in the vertical direction.

The reflectometer may be rotated about the beam line axis to make measurements at either polarization. In the vertical position, the light is p-polarized at a value of about 90% for wavelengths near 130 Angstroms.

For recording the intensity of the light, the reflectometer is instrumented currently with 2 detectors, and either can be used without breaking vacuum. Most measurements, including those reported here, were made using a Hamamatsu GaAsP Schottky photodiode G1127-02 whose window has been removed and which operates in current mode. At low light levels, a pulse-counting channeltron is available for measurement. The detectors are mounted on a trolley which moves along a crescent, allowing them to travel perpendicular (altitude) to the θ-2θ plane at a fixed distance from the sample. The sample angle (θ), detector angle (2θ), and altitude may all be set independently.

A slit is available to cover the photodiode, and its use is required to separate orders when measuring the response of gratings. Although not required for reflectance measurements, the detector slit was used in the measurements reported here as an aid in the determination of any misalignment within the reflectometer. The slit dimensions are 1 mm in the horizontal direction and 4 mm in the vertical direction. At the detector orbit distance of 6 inches, this corresponds to a FWHM of 0.4° x 1.5°.

The detector output is routed using shielded cable to a vacuum feedthru in the wall of the reflectometer, and then into subsequent processing electronics, which digitize the signal and feed it to a COMPAQ 386 PC. This computer is used both to acquire, process, store, and plot the data and to command the reflectometer and monochromator motions and operation before, during, and after data acquisition. (In addition, both the monochromator and reflectometer may be controlled manually using hand-control pods.)

MEASUREMENT PROCEDURE

Using an insertion rod, samples are tranported into the reflectometer from a transfer chamber, while both are under vacuum, and then slid horizontally into the reflectometer's sample holder. Samples are usually positioned so that their center, as determined by eye from fiducials on the sample holder, would be illuminated by synchrotron radiation at normal incidence.

After insertion, the alignment of the sample in the reflectometer may be checked (optionally) using undispersed synchrotron radiation (white light) from the monochromator. To reduce the intensity of white light incident on the photodiode to acceptable levels (of order microamps), a beam line valve (V5) is closed upstream of the exit slit. This valve has a sapphire window of thickness 1 mm which has the effect of cutting off the high-energy spectral component, so that only visible and ultraviolet light are admitted to the reflectometer. The alignment procedure itself consists of several tasks:
(a) Setting the detector at the exact location (in 2θ) of the direct beam so as to initialize this position as 0°. Provision has been made to measure the direct beam by retracting the sample holder slightly. At all other times the sample holder is not retracted, and ideally it then cuts off one half of the direct beam when the sample angle is at 0° grazing angle. This results in a 50% decrease in the recorded intensity.
(b) Rotating the sample and detector in a θ-2θ configuration to a typical grazing angle of 80°. During this motion, the user usually monitors how well the θ-2θ configuration is maintained by observing the visible light reflected off the sample onto the detector slit.
(c) Rotating the sample so that the reflected beam returns upstream through the exit slit assembly. This sample angle (θ) is then initialized as 90°. If the sample is tilted in its holder, the reflected beam may be located above or below the θ-2θ plane. Thus any required motion of the detector in this direction (altitude) is determined also.
(d) Rotating the sample and detector back to 0° grazing angle while monitoring the θ-2θ configuration.

The photodiode is sensitive to visible light so the reflectometer viewports are then covered, and extraneous sources of light such as ion-gauge filaments are turned off. This allows sensitive measurements to be made at the sub-pA level. The background dark current level can be determined by temporarily closing a shutter which is located just upstream of beam line valve V4.

At this point the monochromator is prepared for operation at user-selected wavelengths, and the sapphire window valve V5 is opened. The user selects one filter by translating it into the beam, while the direct beam current is monitored by the detector to identify which filter

is selected. This identification may be verified by scanning the monochromator through an energy range which brackets a filter edge, as the intensity of direct beam light transmitted through the filter is monitored and plotted as a function of energy. (An additional filter, presently Boron, is located in an valve (V4) upstream of the exit slit, thus allowing dual-filter measurements.)

The software routines allow the user to scan the monochromator in energy as data is being taken. A scan of the direct beam is labelled I0. The software also will divide one scan by another (I1) during data acquisition, provided that data points in both scans have the same range and spacing in energy. Thus, the transmission of any filter can be determined by dividing a scan with the filter by one without the filter. By comparing such a "ratio" scan (I1) with a scan made without dividing by I0 (but using the filter), the contribution of higher-order monochromator light may be determined in the I0 beam. This evaluation of "contamination" is valid rigorously only over the energy range selected for the scan. As a check, the measured values from the I1 scan and the edge-ratio can be compared also to theoretical values determined for the known thickness and composition of the filter.

The filter-edge scans also serve to calibrate the energy scale, as the computer software small adjustments that serve to compensate for small misalignments in the monochromator elements by shifting the calculated energy scale. Subsequent energy scans are made to determine the new measured edge energy, and the procedure is repeated until the measured energy of a filter edge matches published values.

Upon filter selection, the user performs one last crucial adjustment before beginning sample measurements. This involves adjusting a parabolic mirror which collimates the beam from the monochromator and focuses this radiation onto the exit slit. This mirror is rolled about an axis parallel to the beam using a hand-control pod, which has the effect of translating the beam horizontally upon the exit slit. The roll angle that allows the radiation to go through the exit slit is a sensitive function of energy. The purpose of this maneuver is to maximize the flux at the energy range of interest, thus providing the ability to make sensitive measurements. Depending upon monochromator elements and settings, substantial gains in flux can be achieved.

The actual reflectance measurements are somewhat simpler than the setup procedure described above and consist of 5 basic parts:

(a) Measure the I0 beam by scanning the monochromator over a desired range in energy around the value at which the roll of the parabolic mirror was optimized. This is done with the detector positioned at an angle of 0° and the sample retracted.

(b) Rotate the sample and detector in a θ-2θ configuration to the desired grazing angle of incidence, for this study 80°.

(c) Move the detector any predetermined distance in altitude to compensate for out-of-plane reflection caused by a tilt of the sample in its holder.
(d) Rotate the detector (2θ) independently of the sample to maximize the signal reflected into the detector slit by compensating for any misalignment.
(e) Measure the I1 reflected beam by scanning the monochromator over the same range and step size used for the I0 measurement, and produce a ratio file (I1), where the data represent the measured reflectance.

At that point the sample and detector are returned to 0° and the procedure may be repeated for different angles of incidence, energy ranges, etc.

POTENTIAL SOURCES OF UNCERTAINTY

There are a number of potential sources of uncertainty, and they may be divided conveniently by location, namely those within the reflectometer, those within X24C and upstream of the reflectometer, and those within the storage ring. Each of these regions is discussed in detail below.

Reflectometer

Perhaps the largest potential source of measurement uncertainty comes from the reflectometer. Errors in alignment, accuracy, and reproducibility can all contribute to angular error which, in turn, leads to uncertainty in the measured reflectance. A few sources are important only when remeasuring samples, where changes with time are being investigated. Most are relevant for both new measurements and remeasurement.

Alignment

Misalignment is a problem for both new and old samples. The two experimental chambers must time-share the beam line and are swapped roughly once a month. The reflectometer has been prealigned and contains alignment fixtures which match hard points fixed on the beam line beneath the exit slit. Thus when the reflectometer is mated to the beam line, alignment should be maintained to a precision of less than 1 mm. This means that when the sample holder is not retracted, one half (ideally) of the synchrotron beam at 0° grazing angle will be blocked by the sample holder, and the other half skirts the surface of the sample in its holder and bisects it vertically. This ensures that the sample axis of rotation (θ) lies along the beam line. To achieve this high degree of alignment the reflectometer has three kinematic points which define a vertical plane (reflectometer vertical) which includes the beam line axis when properly aligned. The sample holder is pushed with a strong spring mechanism so that the sample surface contacts these points. If the reflectometer alignment

is disturbed when the chamber is off-line or during mating/demating operations, provision has been made for realignment. The experimental chamber has the capability of being translated vertically, translated horizontally in a direction perpendicular to the beam line axis, and rotated from vertical to horizontal with respect to its mounting frame.

The sample alignment check procedure described in the previous section is performed generally at least once every time the reflectometer is mated to the beam line. Alignment errors translate into angular errors within the reflectometer. That is, because the zero-point of the detector motion (2θ) is defined by the direct beam and the zero-point of the sample (θ) is defined by the exit slit, misalignment will produce disagreement between these two angles when operated in a θ-2θ configuration, resulting in the reflected beam missing the detector slit. The magnitude of this disagreement is a complex and not fully understood function of the offset between the sample rotation axis and the beam line axis. The largest observed angular misalignment at normal incidence was of order 1 degree, and this was corrected with a translation of 4 mm in the reflectometer perpendicular to the beam line axis. Given the beam size, it is estimated that offsets as small as 0.5 mm can be detected, and this corresponds to an angular error of about 0.1°.

When confronted with a detectable misalignment, the user may choose either to accept the angular error as an uncertainty in the knowledge of the exact angle of incidence or to realign the reflectometer. Given the complications involved in the latter, most users opt for the former. This is not a bad choice when the exact value of the angle of incidence is not important, such as for new samples measured at normal incidence. However, for grazing incidence measurements or when the sample is being remeasured, realignment is preferable, if not mandatory.

A final source of uncertainty arises from the location of the sample holder in the reflectometer. This effect is important only for remeasurement of samples at normal incidence as they may not have uniform response on a size comparable to the beam footprint. At shallow grazing angles the beam footprint is large, and therefore the resulting reflected beam integrates over a large fraction of the surface. The estimated uncertainty in positioning the sample to its center is 0.5 mm, which is half the beam's horizontal width at normal incidence.

Accuracy

Accuracy and reproducibility are strong functions of the reflectometer's angular drive mechanisms. In Hunter & Rife (1986), the quoted precision of the stepping motors was 0.005° and initial measurements resulted in a maximium error of 0.02° in the sample angle of incidence. However, the "wobble stick" rotary motion mechanisms that drove the worm gears suffered from a lack of reproducibility. Therefore these mechanisms have been replaced by steel belt drives. The accuracy of this new system has not been measured yet, but is

believed to be much better than the minimum angular precision that may be commanded by the computer's software, currently 0.05° for θ, 2θ, and the altitude. In practise, users generally set angles with a precision of 0.1°.

Reproducibility

Angular backlash is a common problem that limits reproducibility in such systems. As viewed from above, θ and 2θ increase going counter-clockwise, whereas altitude increases vertically. Computer software has been written to take out the effects of backlash regardless of the user-commanded direction, so that the mechanism always approaches its end destination from the same direction (e.g., counter-clockwise for θ and 2θ). Together with the new steel belt drive mechanisms this software has led to a great improvement in reproducibility. From monitoring of the detector output obtained from repeated motions to the same location, the estimated reproducibility of all angles (θ, 2θ, altitude) is +/- 0.1°.

X24C

The filter mechanism can introduce two types of uncertainty which are potentially important in cases of remeasurement. First, the typical quoted error in the thickness of a given filter is 10%, although the difference between filters made in the same run is somewhat less. However, this means that filters of identical composition and the same nominal thickness may produce slightly different results. Filter transmission at the energy of interest is not the cause of this effect, as the filter is present for both I0 and I1 scans and its transmission divides out. Rather differences may result because the proportion of high-order contamination also varies with filter thickness (as judged by the edge-ratio). However, for the energy range and monochomator settings used for this study, the contribution from higher order radiation is known to be small, and that impact is reduced further by the exponential form of the filter transmission equation. Therefore the total effect on any remeasurement of reflectance in this study is expected to be negligible.

Second, each filter is 5 mm in height, a few times that of the largest aperture selectable with the adjustable slit jaws. This is desirable as it allows the user to position any filter so that its holder does not occult any light incident on the exit slit, but it has the disadvatage that the exact location of the beam footprint on the filter is not known. Hence that position cannot be reproduced for any sample remeasurement. However, the variation in filter thickness with position is quoted typically as a few percent by filter manufacturers, and the beam integrates over a sizeable fraction of the filter area. Thus, the total effect on any remeasurement of reflectance is thought to be negligible again.

Finally, filters may also develop pinholes which allow a higher proportion of high-order contamination through. The appearance of pinholes may be deduced if the edge-ratio of

a filter scan is reduced significantly compared to past results obtained with the same filter or to theoretical values. Users are usually well aware of the expected edge-ratios for X24C beam line filters.

Upstream of the filter assembly lies the steerable parabolic condensing mirror, the monochromator, and another fixed parabolic collimating mirror. The only possible source of error from any of these components would be caused by a change in their properties in between the I0 and I1 measurements. In principle, there should be no changes in the monochromator. However, the motor controlling the roll angle of the steerable mirror is turned off after adjustment so as to prevent crosstalk in the motor-controllers' common power supply from causing a change in the mirror's attitude. The first optical element intercepting the synchrotron radiation is the fixed parabolic collimating mirror. The radiation is intense at its location, and this could cause the mirror to heat up, leading to a change in its figure. Therefore, this mirror is provided with a water cooling system to maintain temperature equilibrium. When the beam line safety shutter is first opened the temperature on this mirror rises from ambient (21-22 °C) to a value (<31 °C) which depends upon the synchrotron ring current. This "warmup" period lasts about 20 minutes, after which measurements can be done without large changes occuring quickly. However, as the synchrotron ring current slowly decays, the temperature of the fixed mirror decreases.

A monitor detector, consisting of a 90% transparent mesh and a current diode, has been installed recently at the exit slit. When the output from this device is integrated fully into the data acquisition program, time variation in the X24C optics will no longer be a source of error.

Storage ring

Of the two known potential sources of error which might be caused by the storage ring, one is accounted for and the other is not. First, the ring current decays exponentially from typical values of 240 mA at injection to 100 mA before dump/reinjection some 12-16 hours later. The X24C computer receives a signal from the synchrotron control room which contains the instantaneous value of the ring current. These values are stored in data files as well as the raw detector signal from the reflectometer. The reflectance calculation takes both signals into account and produces a value that is independent of the time decay of the ring current. Also, real-time current-vs-energy plots that are displayed to the user terminal are normalized to 100 mA beam current.

Second, the electron beam may not be stable in position during any given injection period, and the precise location of the beam in the ring at the X24C port may vary between injections or when orbit "corrections" are made. The effect of this on measurements is not well known, but may result in a small misalignment as the beam line axis is defined by

the exit slit and reflections off the monochromator and mirror elements. Practical time and schedule limitations prevent rechecking alignment after every orbit correction or reinjection. Orbit corrections are rare, but are always announced by the control room. During such times data are not taken. To accomodate the possibility of a small misalignments caused by orbit position, I1 scans are always paired with contemporaneous I0 scans, never those made during a previous injection or before an orbit correction.

MEASUREMENTS

A series of measurements on the test sample was designed to address and quantify what are believed to be the largest sources of uncertainty identified in the previous section. Because this sample had been measured before and a large well-documented data base of results existed, this provided sensitivity to issues of remeasurement.

The measurements occured over a two-day period. On the first day, the sample was inserted and a complete alignment check procedure was done. This revealed a reflectometer misalignment of a magnitude 1° in the detector angle (2θ). It was decided not to realign the reflectometer so that the effect of misalignment could be quantified by comparing the present results with the wealth of previous results for the sample. An I1 scan of the silicon filter L-edge produced a transmission of 39% on the low-energy side of the edge and an edge-ratio of 5:1, in good agreement with past results for this filter. However, the edge occured at a value of 98.6 eV rather than the published value of 100 eV. Therefore the energy scale was adjusted so that a followup scan showed the edge at 99.4 eV. This was judged acceptable for this study as the energy scale can always be shifted linearly during data analysis. The mirror roll was optimized for 95.4 eV, the expected peak value of the multilayer response at a grazing angle 80°. Then one set (I0,I1) of reflectance measurements was made before concluding operations for that day. Normally the monochromator is powered down at the end of a day's work. However, to prevent the possibility that cycling the power might change its condition, the monochromator was left in a power-on state.

On the second day, measurements resumed shortly after beam injection, beam line warmup, and re-optimizing the mirror roll for 95.4 eV. Nine sets of measurments were made in immediate succession without changing any paramameters, each taking about 35 minutes. A tenth set was done after re-optimizing the mirror roll.

Table 1 is a log of the measurements. Column (1) gives the number of the measurement set (I0,I1) with the set measured on the first day labelled as zero. Column (2) gives the peak reflectance of the multilayer in percent, and Column (3) gives the peak energy in eV. Column (4) gives the synchrotron ring current in mA at the beginning of each set. Column (5) gives

the temperature in °C of the fixed parabolic mirror as determined by a thermocouple which is mounted on the back of the mirror holder.

ANALYSIS AND RESULTS

I0 measurements

Flux

The presence of any time variations in X24C and/or the synchrotron can be deduced by examining the eleven I0 files. Figure 1(a) is a plot of I0 curves taken from set 1 and from set 9. At 95 eV and 100-101 eV the two curves overlap. However, at energies less than 95 eV the flux increases with time, while at higher energies the flux decreases. (Note that the direct beam location, 2θ=0, was verified in between each set of measurements.) The largest difference occurs at 85 eV where the flux from I0-9 is 17% greater than the flux from I0-1. As these plots are normalized to 100 mA of the ring current, the time dependent decay of the beam intensity is not the cause of this difference. Data from I0 curves in sets 2 through 8 generally lie incrementally between the two extremes in Figure 1(a). Thus, the shape of the spectrum correlates well with the temperature of the fixed parabolic mirror and with the synchrotron ring current (Table 1).

Figure 1(b) is a plot of I0-9 and I0-10, where the mirror roll angle was re-optimized in between these measurements. This act has changed the spectral shape yet again but in a different fashion, as the flux in I0-10 is higher than that in I0-9 at energies greater than 92 eV and lower elsewhere. The maximum difference of 6% is again at 85 eV.

It is interesting that I0-10 and I0-0 (done the day before) are of similar shape as shown in Figure 1(c). The roll angle adjustments for these scans were made at a similar ring current, although a beam injection also occured between them. The larger flux at energies less than 100 eV in the I0-0 data agrees with the trend seen in Figure 1(a). This suggests that the spectrum shape is correlated strongly with both ring current and mirror roll angle. However, it remains to be proven whether these spectra can be reproduced consistently over many injection cycles for given values of the ring current and mirror roll angle.

The root cause of the time variation of flux and spectral shape in Figure 1(a) is not known. It is tempting to ascribe the effect to changes in the figure of the fixed parabolic collimating mirror, because its temperature changes with the ring current also. However, a correlation does not imply causality. In fact, for several reasons the fixed parabolic collimating mirror is unlikely to be the cause. First, the mirror is made of aluminum which conducts heat efficienctly. Second, the cooling loop extends over the entire length of the

mirror holder, and the mirror is in good thermal contact with its holder and the holder with the cooling loop. Third, the electron beam fills a large fraction of the mirror. In conclusion, the fixed parabolic collimating mirror is likely to be isothermal, and this condition would not lead to a change in its figure.

Another possibility is that the location of the electron beam at the X24C port changes slightly as the beam intensity decays. Small changes in beam position have been noted at other beam line exit ports and on control room monitors. However, the position of the beam at the X24C port is not monitored. Therefore it is not possible currently to verify or deny this hypothesis.

For now, it is possible only to quantify the effect that the observed time variation in the incident beam has on measurements. The maximum flux change of 17% at 85 eV occured over 9 measurement sets, for an average of 2% per data set (I0,I1). Therefore, the relative difference in flux between I0 and I1 is about 1% leading to a maximum relative error of 1% in the reflectance. If it turns out that the spectral shape is a reproducible function of ring current and mirror roll angle, this error becomes an offset and may be calibrated out. However, until then it remains as a maximum contribution to the uncertainty of 1% of the value of the reflectance. As an average contribution over all energies in Figure 1(a), a value of 0.4% was calculated.

The arguments presented above have assumed that no time-dependent changes occur downstream of the exit slit, in the reflectometer, the detector, or the processing electronics. There are no processes known to us that could cause the reflectometer or processing electronics to change on the timescales of these measurements. However, detector changes, although unlikely, are possible. Certainly the implementation of the I0 current monitor at the exit slit would help to locate the source of any changes within X24C, and more measurements should be made.

Energy scale

Examination of the position of the silicon L-edge in all eleven plots suggests that there is no systematic variation in the measured energy of the edge. However, a slight random variation in the measured energy of points with equal flux is observed near the edge. The bin size is 0.2 eV and the observed variation is about half this value or 0.1 eV. To this uncertainty, another contribution of 0.2 eV is added in quadrature to account for uncertainty in the calibration constants used to correct for small misalignments in the monochromator elements. Thus, the total uncertainty in the energy scale at 100 eV is 0.22 eV, which corresponds to a total uncertainty of about 0.3 Angstroms in the wavelength scale. Note that this uncertainty is smaller than the offset between the measured energy of the silicon L-edge and published values.

I1 measurements

In Figure 2(a), I1 scans are plotted from measurement sets 1 and 9. Plots of I1 scans from intermediate sets lie within these extremes. There is a visible shift of the main multilayer peak to lower energies, and the peak reflectance drops about 1% from 43.5% to 42.6%. Note the trend in Table 1 for the peak reflectance to decrease in going from set 1 to set 9. These results are consistent with the progressive change in flux that was determined for the direct beam and which causes the incident flux to be slightly different from the I0 measurement when the I1 measurement is made. However, the **relative** decrease of over 2% of the peak reflectance value is twice that expected from just the change in the incident beam.

In Figure 2(b), the I1-10 scan made after re-optimizing the mirror roll angle is compared with the I1-9 scan. The act of re-optimizing the roll angle has restored the value of the peak reflectance. This suggests that measurements should be made shortly after optimizing the mirror roll angle. It is not standard procedure for a user to re-optimize the mirror roll angle immediately before every set of measurements. Therefore, a conservative estimate of the measuremental uncertainty in reflectance as a function of energy may be determined by averaging the I1 data for sets 1 through 9 at each energy point. The energy bin closest to the average peak energy is 95.4 eV (Table 1), and the average peak reflectance there is 43.12% +/- 0.44%. Figure 3(a) is the standard deviation on this average plotted as a function of energy. The standard deviation of the peak energy resides in a relative minimum. The locations of minima and maxima in this Figure 3(a) are correlated strongly with the slope of the reflectance profile (Figure 2), a reasonable result given the energy shift discussed above. The maximum standard deviation is about 1.5% near the steep slope in reflectance at the half-maximum energies of the main multilayer peak. However, typical values range from 0.1 to 0.5%.

In Figure 3(b), the standard deviation profile in Figure 3(a) is divided by the average reflectance profile. At most energies, the standard deviation ranges from 1 to 10-20% of the reflectance. As expected, it is also anti-correlated with reflectance so that this **relative** standard deviation is small at energies where the reflectance, and hence the signal-to-noise, is large. However, where the signal-to-noise is low as, for example, at energies greater than the silicon L-edge (100 eV), the uncertainty in the measured reflectance may be comparable to the value of the measured reflectance.

The peak energy agrees well with the data base of results from previous measurements which suggests that the either the reflectometer misalignment had a negligible effect on the results or that the previous measurements were made with similar degrees of misalignment in the reflectometer. The average peak reflectance is about 2 standard deviations higher than obtained during the last series of measurements, some 3 months earlier. Although

this difference is of marginal statistical significance, there are at least three possible explanations. First would be the precision and reproducibility uncertainties associated with the reflectometer. Second, the sample may not have been positioned precisely at its center, and the new beam footprint (of horizontal width 1 mm) is located up to 0.5 mm from the center on a more efficient region of the sample. Third, the test sample was subject to X-ray photoelectron spectroscopy measurements during the interim between the last series of reflectance measurements and the present study. Although photoelectron spectroscopy is not thought to affect the sample surface, the possibility remains that some of the carbon contamination was cleaned away.

DISCUSSION

The results from these tests are a promising start in understanding measuremental uncertainty. However, they span a rather small subset of the available parameter space of measurement. A complete examination would require: (a) tests throughout the entire energy range of the monochromator and with all the different grating elements and corresponding choices of filter, (b) tests using different samples such as single films, gratings, and multilayers with different bandpasses, and (c) tests at different angles of incidence from grazing to normal and at S-polarization (reflectometer horizontal). Such a test program would be a monumental effort. However, in lieu of all that, we can extrapolate with good confidence the present results to other parameter domains, some of which are discussed below.

Low signal-to-noise measurements

The direct beam flux at the test sample's peak energy (95.4 eV) was of order tens of nanoamps and the dark current during the I0 measurments was approximately 0.1 picoamp. However because the reflectance was high, the measured current for the reflected beam was still many orders of magnitude greater than the background dark current. Therefore the dark current could be ignored in the reflectance calculation. In cases where the reflectance (efficiency) and/or the incident flux is low, the signal-to-noise of the reflected beam may be poor and measuremental uncertainties will be large unless the dark current is taken into account. The software does provides the capability to subtract a user-provided DC dark current from measured values. The causes of the dark current are not fully known, but it is known, for example, that the dark current varies with the position of the detector (2θ) in the reflectometer. Hence the dark current should be determined separately for the I0 and I1 scans.

The presence of any AC component to the dark current complicates matters in the low signal-to-noise domain in the same manner as the systematic time variations in the direct

beam that were discussed in the previous sections. However, as mentioned, an estimate of both the AC and the DC components of the dark current may be obtained by temporarily closing a shutter on the beam line. Figure 4(a) shows the measured dark current with the detector located at the position of the reflected beam. To produce a plot, the software requires that either the monochromator be scanned in energy or the reflectometer be scanned in angle. (A time-scan mode has not been coded.) The former was selected which leads to an energy label for the abscissa. However, as a shutter is closed between the monochromator and the reflectometer, the abscissa is really a time axis. In Figure 4(a), the DC level of the dark current is 0.037 pA, a typical value. The dark current profile is also relatively flat which indicates there is no strong drift in the DC level on the time scale of the scan (about 2 minutes), as expected. There is statistical jitter (AC) in the dark current at a level of 0.007 pA RMS.

In Figure 4(b), the dark current and the reflected current profile are plotted together as a function of 2θ. The sample was a multilayer-coated grating, and the scan was done at an energy of 627 eV with the grazing angle held fixed at 21.6°. The computer varied the position in (2θ) of the detector, and to avoid transients caused by the motion, the computer stopped the detector at each location for 1 second before accumulating data. The zero order and first outside order peaks are clearly visible in Figure 4(b) at 42° and 43°, respectively. However, at angles of 2θ less than 41° and greater than 43°, the dark and reflected current profiles are nearly identical. Moreover, the dark current profile has a great deal of structure and reaches a rather high current of about 1 pA near the center of the plot at the θ-2θ configuration. It was found that this result was reproducible, but the causes of this structure are not known. We speculate that capacitive coupling between the signal cable and parts within the reflectometer might be one cause, although the signal cable is shielded. Alternatively, ground loop currents and charging of parts within the reflectometer are other possibilities.

To date, correlations have been noted between the dark current and the values of θ, 2θ, and the readout scale chosen for the electrometer which receives the signal from the diode detector. A complete examination is clearly desirable. However, it does appear possible to determine both the DC and AC components for any set of conditions. If so, there will be no increase in measurement uncertainty even in low signal-to-noise cases if the dark current levels are measured and subtracted off properly.

Measurements at non-normal angles of incidence

Angular uncertainty has been examined at only a few angles of incidence from grazing to normal. However, the reproducibility appears to be uniform at +/− 0.1°. Thus, it is likely that measuremental uncertainty should be independent of most angles of incidence. At shallow angles of incidence, misalignment could produce a large uncertainty, and this

effect should be quantified. In addition, the horizontal width of the incident beam on the sample is large, and therefore care must be taken in positioning the sample so that the beam does not "spill over". This would result in an underestimate of the reflectance (efficiency). Sample holders generally limit the sample horizontal width to 1 inch, and spill over occurs at grazing angles less than 2.3°.

S-polarization measurements

The reflectometer can be rotated to a horizontal position to make measurements at S-polarization. However when this is done, gravity causes a small sag in the crescent which transports the detector in 2θ and altitude, leading to an apparent offset of the reflected beam in 2θ. Thus, white light alignment checks for each new sample are highly recommended. Much less experience has been gained in operation at S-polarization, but it appears that reproducibility and accuracy are comparable to the P-polarization case. Hence, measuremental uncertainty should be similar. In one dark current measurement, made during a detector angular scan, the profile was flat and did not show the structure visible in Figure 4(b). When the slit is used, the I0 measurement should also be made in S-polarization, as the beam footprint may be rectangular rather than square depending upon the width of the exit slit. (However, the detector is not sensitive to polarization.)

CONCLUSIONS

A comprehensive attempt has been made to identify and quantify sources of uncertainty associated with measurements made with the reflectometer on the NRL beam line X24C. A multilayer-coated mirror sample was subjected to a battery of tests. The following conclusions can be drawn:

1. Measurement uncertainty is caused by a combination of factors. The dominant sources appear to be angular reproducibility in the reflectometer and the stability of the electron beam. Sample and reflectometer alignment are less important except in the cases of sample remeasurement. The rotation of the steerable parabolic condensing mirror is critical to optimizing the incident flux, and therefore should never be done between measurement of the direct and reflected beams.

2. At wavelengths near the silicon L edge, the error in wavelength scale is about 0.3 Angstroms.

3. In multilayer samples with good signal-to-noise, the error in the peak reflectance is about 1% of the value of the peak reflectance (e.g., 0.5% for 50% peak reflectance). The error is correlated with the slope of the reflectance profile, varying between 1% of the reflectance

value where the slope is flat to 10% of the reflectance value where the slope is steep. In other samples with flatter profiles, the error in the measured reflectance is expected to stay at about 1% of the value of the reflectance.

4. In samples with low signal-to noise, the background dark current should be measured and subtracted off separately for both the direct and reflected beams. Measuremental uncertainty should not increase if this is done. Similarly, uncertainties should be independent of the sample angle of incidence and the polarization measured.

ACKNOWLEDGEMENTS

This work was supported by the U. S. Office of Naval Research (NRL project 76-3641). Part of the work was carried out at the National Synchrotron Light Source, which is sponsored by the U. S. Department of Energy under contract DEAC02-76CH00016.

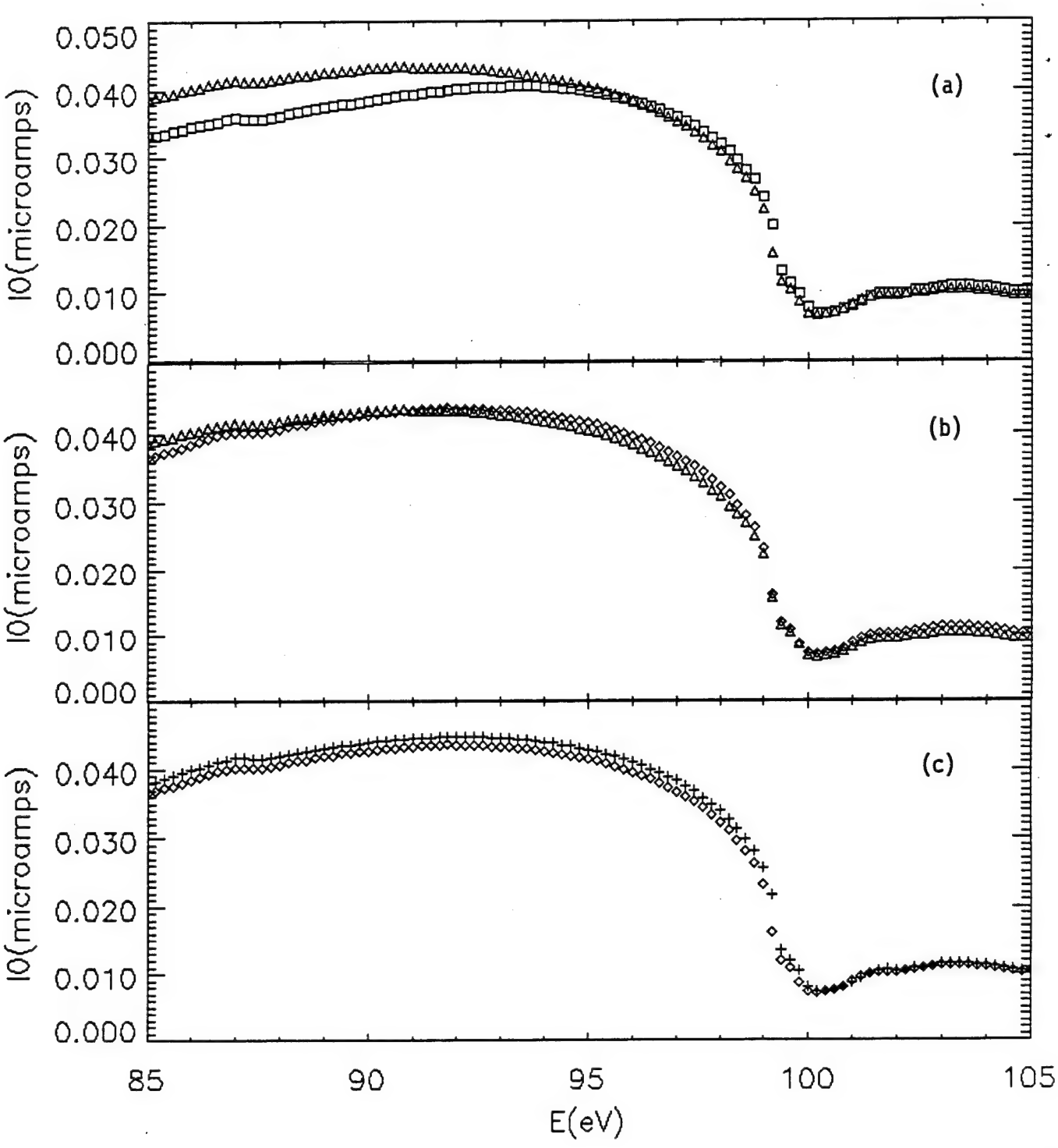

Figure 1 — I0 Measurements. (a) Data from set 1 (squares) and set 9 (triangles). (b) Data from set 9 (triangles) and set 10 (diamonds). (c) Data from set 10 (diamonds) and set 0 (plus signs).

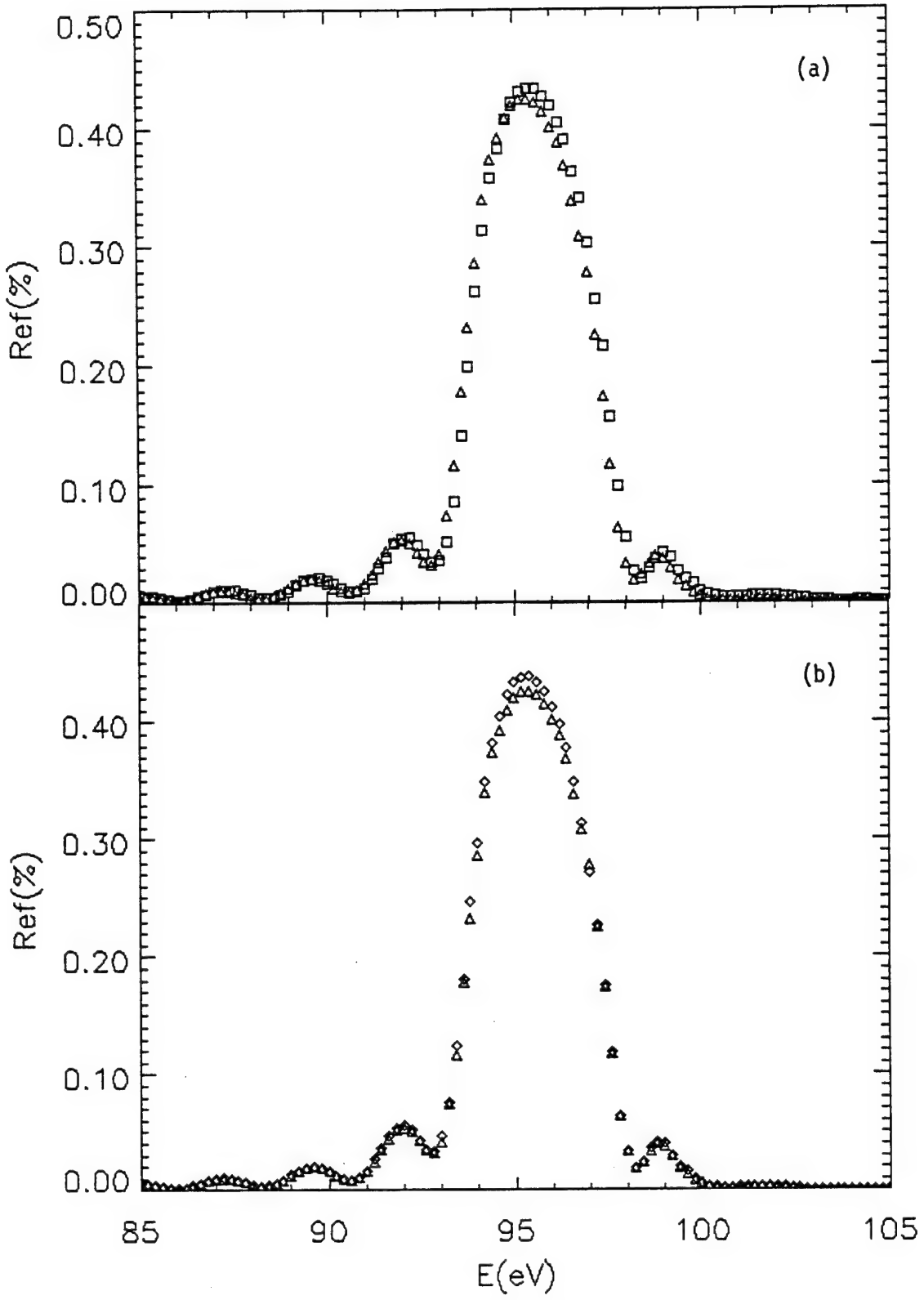

Figure 2 — I1 Measurements. (a) Data from set 1 (squares) and set 9 (triangles). (b) Data from set 9 (triangles) and set 10 (diamonds).

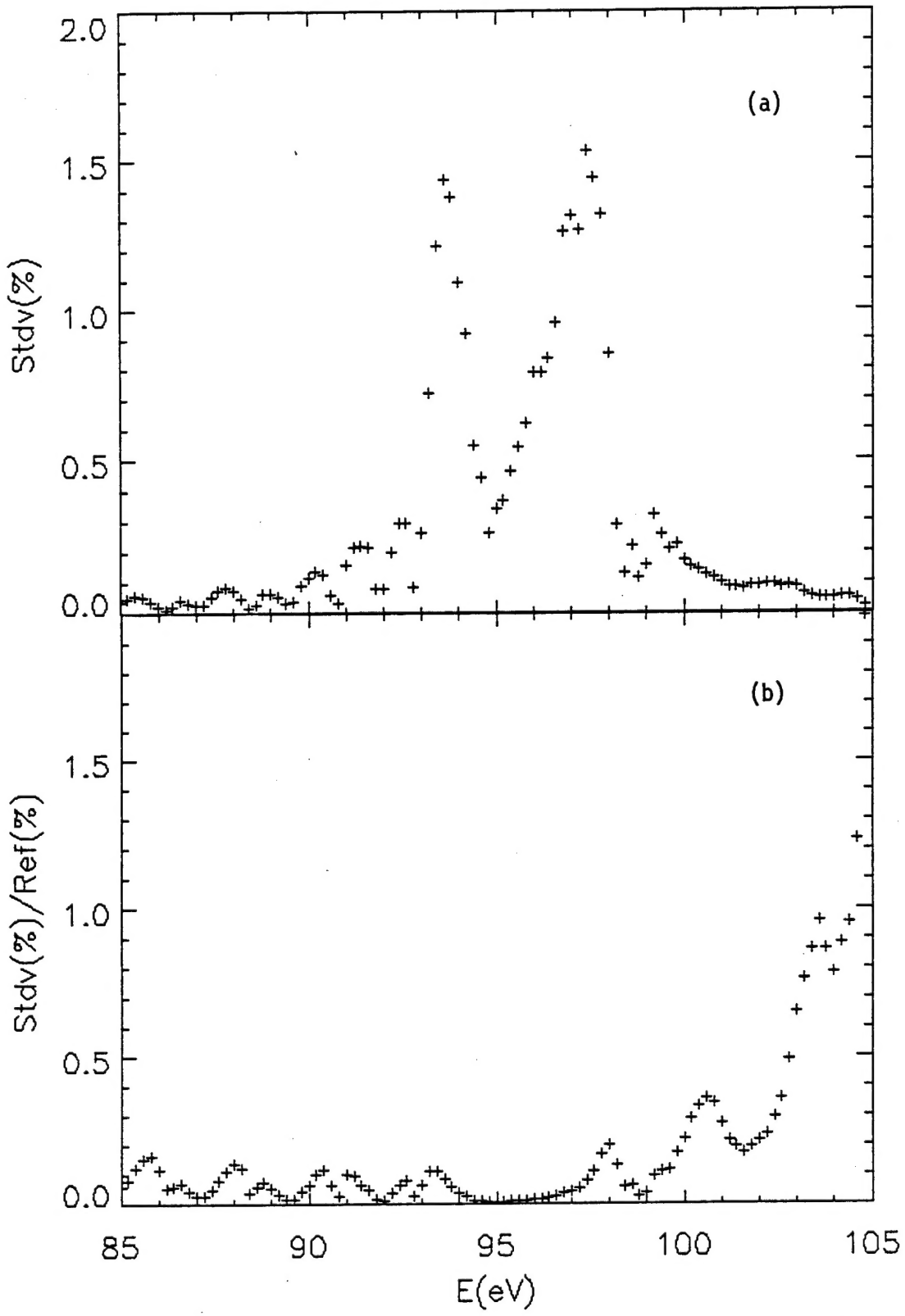

Figure 3 — Standard Deviation. (a) The standard deviation of the measured reflectance for the average of sets 1-9. (b) The **relative** standard deviation obtained by dividing the result in (a) by the average measured reflectance.

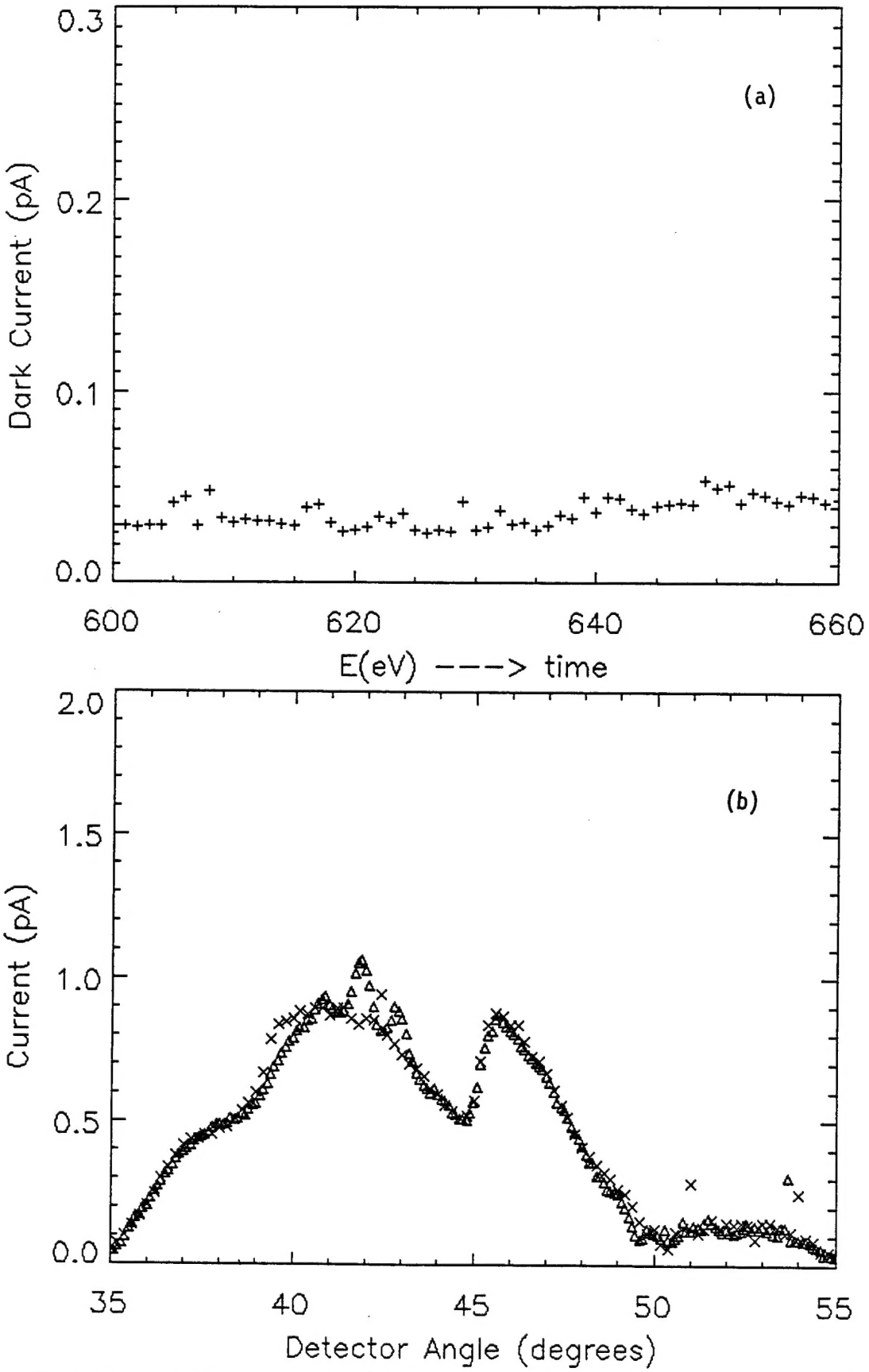

Figure 4 — Dark Current Measurements. (a) Data were taken during an energy scan, but with a beam line shutter closed. (b) Crosses indicate data taken during a scan in 2θ with the beam line shutter closed. Triangles indicate data taken with the beam line shutter open.

REFERENCES

T. W. Barbee, Jr., J. C. Rife, W. R. Hunter, M. P. Kowalski, R. G. Cruddace, & J. F. Seely, *Applied Optics*, **32**, 4852 (1993).

T. -J. Chen, & W. R. Hunter, in preparation (1995).

R. G. Cruddace, T. W. Barbee, Jr., J. C. Rife, & W. R. Hunter, *Physica Scripta*, **41**, 396 (1990).

W. R. Hunter, & J. C. Rife, *Nuclear Instruments and Methods in Physics Research*, **A246**, 465 (1986).

M. P. Kowalski, J. F. Seely, W. R. Hunter, J. C. Rife, T. W. Barbee, Jr., G. E. Holland, C. N. Boyer, & R. G. Cruddace, *Applied Optics*, **32**, 2422 (1993).

M. P. Kowalski, T. W. Barbee, Jr., R. G. Cruddace, J. F. Seely, J. C. Rife, & W. R. Hunter, *Applied Optics*, in preparation (1995).

J. C. Rife, W. R. Hunter, & R. T. Williams, *Nuclear Instruments and Methods in Physics Research*, **A246**, 252 (1986).

J. C. Rife, H. R. Sadeghi, & W. R. Hunter, *Review of Scientific Instruments*, **60**, 2064 (1989).

S. E. Schnatterly, et al., in preparation (1995).

J. F. Seely, G. Gutman, J. Wood, G. S. Herman, M. P. Kowalski, J. C. Rife, & W. R. Hunter, *Applied Optics*, **32**, 3541 (1993a).

J. F. Seely, M. P. Kowalski, W. R. Hunter, J. C. Rife, T. W. Barbee, Jr., G. E. Holland, C. N. Boyer, & C. M. Brown, *Applied Optics*, **32**, 4890 (1993b).

J. F. Seely, W. R. Hunter, J. C. Rife, & M. P. Kowalski, *Applied Optics*, **31**, 7367 (1992).

TABLE 1
Log of Measurements

Set	Ref (%)	Energy (eV)	Current (mA)	Temperature (°C)
(1)	(2)	(3)	(4)	(5)
0	42.8	95.4	156	26
1	43.5	95.4	225	29
2	43.9	95.4	220	29
3	43.4	95.4	214	29
4	42.8	95.4	208	29
5	43.1	95.2	202	29
6	43.3	95.4	197	29
7	42.6	95.2	192	29
8	42.9	95.4	187	28
9	42.6	95.4	183	28
10	43.8	95.4	178	28